One-Loop Dominance in the Imaginary Part of the Polarizability: Application to Blackbody and Noncontact van der Waals Friction

U. D. Jentschura,[1,*] G. Łach,[2,3] M. De Kieviet,[4] and K. Pachucki[3]
[1]Department of Physics, Missouri University of Science and Technology, Rolla, Missouri 65409, USA
[2]International Institute of Molecular and Cell Biology, Księcia Trojdena 4, 02-109 Warsaw, Poland
[3]Faculty of Physics, University of Warsaw, Pasteura 5, 02-093 Warsaw, Poland
[4]Klaus-Tschira-Gebäude, Im Neuenheimer Feld 226, 69120 Heidelberg, Germany
(Received 4 September 2014; published 27 January 2015)

Phenomenologically important quantum dissipative processes include blackbody friction (an atom absorbs counterpropagating blueshifted photons and spontaneously emits them in all directions, losing kinetic energy) and noncontact van der Waals friction (in the vicinity of a dielectric surface, the mirror charges of the constituent particles inside the surface experience drag, slowing the atom). The theoretical predictions for these processes are modified upon a rigorous quantum electrodynamic treatment, which shows that the one-loop "correction" yields the dominant contribution to the off-resonant, gauge-invariant, imaginary part of the atom's polarizability at room temperature, for typical atom-surface interactions. The tree-level contribution to the polarizability dominates at high temperature.

DOI: 10.1103/PhysRevLett.114.043001 PACS numbers: 31.30.jh, 12.20.Ds, 31.15.-p

Introduction.—Can a physical object experience friction effects, even if it is not in contact with a surface, i.e., even if the overlap of the wave function of the atom with the surface is negligible? This question has intrigued physicists for the past three decades, and the precise functional form of the noncontact friction of an atom-surface interaction has been discussed controversially in the literature [1–9]. Intuitively, if an ion moves parallel to a surface, at a distance a few (hundred) nanometers, then it is quite natural to assume that the motion of the mirror charge inside the material leads to Ohmic heating and, thus, to a commensurate energy loss (friction force) acting on the atom flying by. The corresponding effect for a neutral atom is less obvious to analyze, but one may argue that the thermal fluctuations of the electric dipole moment of the atom may induce corresponding fluctuations of the mirror charge(s) of the constituent particles of the atom inside the material, again leading to Ohmic heating. The derivation relies heavily on the quantum statistical theory of thermal fluctuations of the electromagnetic field near a surface and on the fluctuation-dissipation theorem [5,10,11]. For noncontact friction in the zero-temperature limit, even the existence of the effect is still subject to scientific debate [12–15]. Ultimately, noncontact friction effects limit the extent to which friction forces [16] can be reduced in an experiment. These limits are important for three-dimensional atomic imaging [17], tests of gravitational interactions at small length scales [18], and limits of magnetic resonance force microscopy [19], and they affect the behavior of MEMS at the nanometer scale [20].

Complementing the effect of noncontact friction, the drag exerted by oncoming blueshifted thermal blackbody radiation on a moving atom has recently been analyzed for nonrelativistic neutral atoms as they travel through space [21–24]. Both the blackbody as well as the noncontact quantum (thermal) friction require as input the imaginary part of the atom's polarizability, whose precise functional form for small driving frequencies is different depending on whether one uses (i) resonant Dirac-δ peaks [21] or the (ii) length-gauge or (iii) velocity-gauge expressions in the low-frequency limit (see Ref. [24] and Chap. XXI of Ref. [25]). Any theoretical prediction crucially depends on a resolution of the "gauge puzzle," which is the subject of this Letter. Quite surprisingly, a separation of the problem in terms of a rigorous quantum electrodynamic approach to the atom [26] leads to a natural separation of the resonant and the nonresonant (one-loop) effects. Perhaps even more surprisingly, the one-loop correction here dominates over the tree-level term, for typical materials and temperatures.

Imaginary part of the polarizability.—The calculation of the imaginary part of the polarizability relies on the following two observations. (i) One identifies the main contribution to the imaginary part of the polarizability with the imaginary part of an energy shift, namely, the ac Stark shift [27]. In second quantization, the ac Stark shift in a laser field can be formulated in terms of the virtual transitions of a reference state (atom in the state $|\phi_0\rangle$ and n_L laser photons) to a virtual state with the atom in the virtual state $|\phi_m\rangle$ and $n_L \pm 1$ laser photons. (ii) One observes that the imaginary part is generated by an additional virtual photon loop (self-energy insertion), which is cut in the middle of the diagram, with a virtual state that brings the atom back to the reference state $|\phi_0\rangle$, has $n_L - 1$ laser photons (one laser photon has been absorbed) and one spontaneously emitted photon, with wave vector $\vec{k}$, polarization λ, and an energy $\omega_{\vec{k}\lambda} = \omega_L$.

 © 2015 American Physical Society

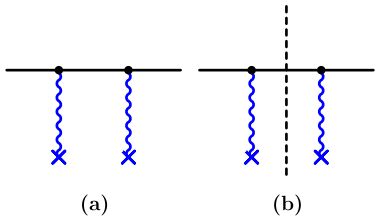

FIG. 1 (color online). The Feynman diagram for the ac Stark shift involves the absorption or emission of two laser photons by the atom (a). A tree-level imaginary part [cut of the diagram, see (b)] is generated only if the absorbed laser photon happens to be at resonance with regard to a transition of the atom to an excited state [see Eq. (12)].

The Feynman diagram for the ac Stark shift is given in Fig. 1. The reference state is $|\phi_0\rangle = |\phi, n_L, 0\rangle$, with the atom in the state $|\phi\rangle$, n_L laser photons, and zero photons in other modes. The energy eigenvalue of the unperturbed reference state is $H_Q|\phi_0\rangle = E_0|\phi_0\rangle$, with $E_0 = E + \hbar n_L \omega_L$, where H_Q is the sum of the atomic (A) and the electromagnetic (EM) field Hamiltonians,

$$H_Q = H_A + H_{\rm EM}, \qquad H_A = \sum_m E_m |\phi_m\rangle\langle\phi_m|, \tag{1a}$$

$$H_{\rm EM} = \sum_{\vec{k}\lambda \neq L} \hbar\omega_{\vec{k}\lambda} a^+_{\vec{k}\lambda} a_{\vec{k}\lambda} + \hbar\omega_L a^+_L a_L, \tag{1b}$$

where L denotes the laser mode, and the photon creation and annihilation operators are a^+ and a, respectively [28,29]. If the laser photon of angular frequency ω_L is resonant with respect to an atomic transition, then the absorption of a laser photon may deplete the reference state, leading to a transition to a state $|\phi_r\rangle = |\phi_m, n_L - 1, 0\rangle$, provided $\hbar\omega_L = E_m - E$, where E is the atomic reference state energy. However, when the absorption of a laser photon is accompanied by the spontaneous emission of another photon, then a transition to a final state $|\phi_f\rangle = |\phi, n_L - 1, 1_{\vec{k}\lambda}\rangle$ becomes possible, where the laser fields retain $n_L - 1$ photons, while one photon is emitted into the mode $\vec{k}\lambda$ (the state is $|1_{\vec{k}\lambda}\rangle$ in the occupation number notation). The imaginary part of the ac Stark shift due to the diagrams in Fig. 2 is due to the dipole interaction H_L (z-polarized laser) and the interaction Hamiltonian H_I (other field modes),

$$\vec{E}_L = \hat{e}_z \sqrt{\frac{\hbar\omega_L}{2\epsilon_0 \mathcal{V}_L}} (a_L + a^+_L) = \hat{e}_z E_L, \tag{2a}$$

$$\vec{E} = \sum_{\vec{k}\lambda} \sqrt{\frac{\hbar\omega_{\vec{k}\lambda}}{2\epsilon_0 \mathcal{V}}} \hat{e}_{\vec{k}\lambda} (a_{\vec{k}\lambda} + a^+_{\vec{k}\lambda}), \tag{2b}$$

$$H_L = -ezE_L, \qquad H_I = -e\vec{r}\cdot\vec{E}. \tag{2c}$$

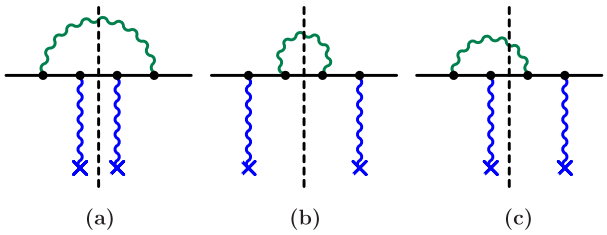

FIG. 2 (color online). The radiative correction to the ac Stark shift involves an additional virtual photon loop (green). The imaginary part (cut of the diagram) is generated when the virtual photon becomes real, i.e., when the laser photon has the same energy as the spontaneously emitted photon. The different insertions of the radiative photon in time-ordered perturbation theory lead to the diagrams in (a)–(c).

Here, the normalization volumes are $\mathcal{V}$ for the quantized field and $\mathcal{V}_L$ for the laser field. We can write

$$I_L = \frac{n_L \hbar\omega_L c}{\mathcal{V}_L}, \qquad \sum_{\vec{k}} = \mathcal{V} \int \frac{d^3k}{(2\pi)^3} \tag{3}$$

for the laser field intensity I_L and the matching of the sum over available photon modes $\sum_{\vec{k}}$ to the integral $\int d^3k$ over the continuum. Second-order perturbation theory for the reference state $|\phi_0\rangle$ leads to [27]

$$\delta E^{(2)} = -\langle H_L G'(E_0) H_L\rangle = -\frac{I_L}{2\epsilon_0 c}\alpha(\omega_L), \tag{4a}$$

$$\begin{aligned}\alpha(\omega_L) &= e^2 \sum_{\pm} \langle\phi|z G_A(E \pm \omega_L) z|\phi\rangle \\ &= \frac{e^2}{3} \sum_{\pm} \langle\phi|x^i G_A(E \pm \omega_L) x^i|\phi\rangle,\end{aligned} \tag{4b}$$

where $G'(z) = [1/(H_Q - z)]'$ is the reduced Green function for atom plus field (with the reference state $|\phi_0\rangle$ excluded), while $G_A(z) = [1/(H_A - z - i\epsilon)]$ is the atomic Green function. The "reduction" of the Green function excludes the combined atom plus field state $|\phi_0\rangle$ but not the atomic reference state $|\phi\rangle$. We assume that the atom's reference state is spherically symmetric. The fourth-order energy shift leads to the diagrams shown in Fig. 2,

$$\begin{aligned}\delta E^{(4)} = &-\langle H_I G'(E_0) H_L G'(E_0) H_L G'(E_0) H_I\rangle \\ &- \langle H_L G'(E_0) H_I G'(E_0) H_I G'(E_0) H_L\rangle \\ &- 2\langle H_I G'(E_0) H_L G'(E_0) H_I G'(E_0) H_L\rangle.\end{aligned} \tag{5}$$

The three terms in Eq. (5) correspond to the diagrams in Figs. 2(a)–2(c), respectively. Let us consider the energy shift due to the diagram in Fig. 2(a),

$$\delta E_a = -e^4 \sum_{\vec{k}\lambda} \frac{\hbar\omega_L}{2\epsilon_0 \mathcal{V}_L} \frac{\hbar\omega_{\vec{k}\lambda}}{2\epsilon_0 \mathcal{V}} \langle\phi_0|(\hat{\epsilon}_{\vec{k}\lambda}\cdot\vec{r})(a^+_{\vec{k}\lambda} + a_{\vec{k}\lambda}) \times G'(E_0) z (a^+_L + a_L) G'(E_0) z (a^+_L + a_L) \times G'(E_0)(\hat{\epsilon}_{\vec{k}\lambda}\cdot\vec{r})(a^+_{\vec{k}\lambda} + a_{\vec{k}\lambda})|\phi_0\rangle. \quad (6)$$

In order to calculate the imaginary part, one isolates the terms that correspond to the absorption from the laser field and emission into the spontaneous mode. Using the matching condition (3) and summing over the polarizations of the spontaneously emitted photon, one obtains

$$\delta E_a \sim -e^4 \int \frac{d^3k}{(2\pi)^3} \frac{I_L}{2\epsilon_0 c} \frac{\hbar\omega_{\vec{k}\lambda}}{2\epsilon_0} \left(\delta^{ij} - \frac{k^i k^j}{\vec{k}^2}\right) \times \langle\phi|z G_A(E-\omega_{\vec{k}\lambda}) x^i G_A(E+\omega_L-\omega_{\vec{k}\lambda}) \times x^j G_A(E-\omega_{\vec{k}\lambda}) z|\phi\rangle. \quad (7)$$

The imaginary part due to the transition into the state $|\phi_f\rangle$ can be extracted from the relation $1/(x-i\epsilon) \to (\mathrm{P.V.})(1/x) + i\pi\delta(x)$, where (P.V.) denotes the principal value, i.e., by projecting

$$G_A(E+\omega_L-\omega_{\vec{k}\lambda}) \to \frac{i\pi}{\hbar}\delta(\omega_{\vec{k}\lambda}-\omega_L)|\phi\rangle\langle\phi|. \quad (8)$$

One finally obtains

$$\mathrm{Im}(\delta E_a) = -\frac{I_L}{2\epsilon_0 c}\frac{\omega_L^3}{6\pi\epsilon_0 c^3}\left[\frac{e^2}{3}\langle\phi|x^i G_A(E-\omega_L)x^i|\phi\rangle\right]^2, \quad (9)$$

and after summing up the diagrams in Figs. 2(a)–2(c), the result is

$$\mathrm{Im}(\delta E^{(4)}) = -\frac{I_L}{2\epsilon_0 c}\frac{\omega_L^3}{6\pi\epsilon_0 c^3}\left[\frac{e^2}{3}\langle\phi|x^i G_A(E-\omega_L)x^i|\phi\rangle + \frac{e^2}{3}\langle\phi|x^j G_A(E+\omega_L)x^j|\phi\rangle\right]^2, \quad (10)$$

so that $\mathrm{Im}(\delta E^{(4)}) = -(I_L/2\epsilon_0 c)\ (\omega_L^3/6\pi\epsilon_0 c^3)[\alpha(\omega_L)]^2$. Matching with the second-order ac Stark shift given in Eq. (4), and adding the resonant contribution [Fig. 1(b)], one obtains

$$\mathrm{Im}[\alpha(\omega_L)] = \mathrm{Im}[\alpha_R(\omega_L)] + \frac{\omega_L^3}{6\pi\epsilon_0 c^3}[\alpha(\omega_L)]^2. \quad (11)$$

Here, $\mathrm{Im}[\alpha_R(\omega_L)] = \mathrm{Im}[\alpha_r(\omega_L)] - \mathrm{Im}[\alpha_r(-\omega_L)]$where

$$\mathrm{Im}[\alpha_r(\omega_L)] = \frac{\pi}{2}\sum_m \frac{f_{m0}}{E_m - E}\delta(E_m - E + \hbar\omega_L) \quad (12)$$

is the resonant contribution. (Both the resonant as well as the nonresonant (one-loop) contributions to the atomic polarizability are odd under a sign change of ω_L, and $E_m - E$ is the angular frequency for the excitation to the excited state of energy E_m.) The dipole oscillator strength f_{m0} reads as $f_{m0} = \frac{2}{3}e^2(E_m - E)|\langle\phi|x^i|\phi_m\rangle|^2$ (see Ref. [30]). The result (11) allows us to unify the formulas given in Eqs. (G2) and (G3) of Ref. [31], Eq. (49) of Ref. [32], and Eq. (15.83) of Ref. [33] into a single, compact result. Namely, the appearance of the square of the polarizability is otherwise ascribed to a radiative reaction force [31,32] but finds a natural interpretation within a QED formalism. The resonant contribution is the tree-level term in QED.

In velocity gauge, one replaces for the dipole coupling $-e\vec{r}\cdot\vec{E}$ by $-e\vec{p}\cdot\vec{A}/m_e$, where m_e is the electron mass. From the diagrams in Fig. 2, one then obtains the energy shift given in Eq. (10), but with the replacement $\omega_L^3 \to \omega_L$ in the prefactor and $x^i \to p^i/m_e$ in the dipole matrix elements. The resulting expression is not identical to the length-gauge result (11), but there are additional diagrams to consider, given in Fig. 3, which involve the seagull Hamiltonian, proportional to the square of the vector potential. Using the commutator relation $p^i = im_e[H - E + \omega_L, r^i]$ repeatedly, one can show that the additional terms from the diagrams in Fig. 3 restore the full gauge invariance of the result (11).

Numerical evaluation.—We are concerned with the numerical evaluation of the blackbody friction integral (restoring SI MKSA units)

$$\eta_{\mathrm{BB}} = \frac{\beta\hbar^2}{12\pi^2\epsilon_0 c^5}\int_0^\infty \frac{d\omega\omega^5 \mathrm{Im}[\alpha(\omega)]}{\sinh^2(\frac{1}{2}\beta\hbar\omega)}, \quad (13)$$

which determines the blackbody radiation force $F = -\eta v$ and the noncontact friction integral (in SI MKSA),

$$\eta_{\mathrm{QF}} = \frac{3\beta\hbar^2}{32\pi^2\epsilon_0 \mathcal{Z}^5}\int_0^\infty \frac{d\omega \mathrm{Im}[\alpha(\omega)]}{\sinh^2(\frac{1}{2}\beta\hbar\omega)}\mathrm{Im}\left[\frac{\epsilon(\omega)-1}{\epsilon(\omega)+1}\right], \quad (14)$$

for interactions with a dielectric. Here, $\beta = 1/(k_B T)$ is the Boltzmann factor, $\mathcal{Z}$ is the distance to the wall, and ϵ_0 is the vacuum permittivity.

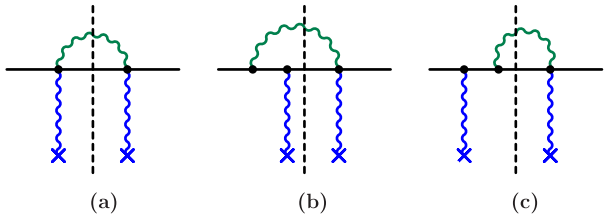

FIG. 3 (color online). In velocity gauge, the seagull term leads to additional diagrams with a two-photon vertex. As in Fig. 2, the different insertions of the radiative photons in time-ordered perturbation theory lead to the diagrams in (a)–(c).

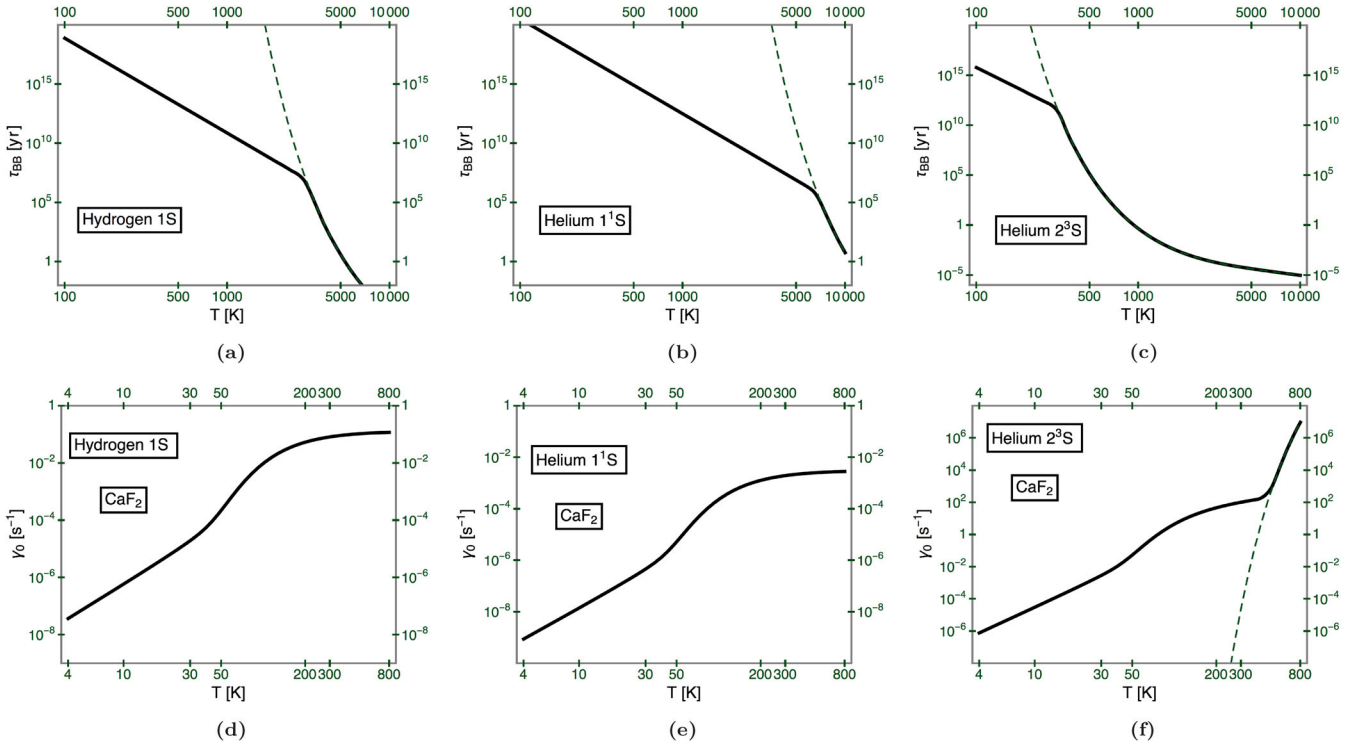

FIG. 4 (color online). Theoretical predictions (a)–(c) for the attenuation time τ_{BB} (equal to the ratio of atomic mass to η_{BB}) are displayed for blackbody radiation friction. For CaF_2 van der Waals friction (d)–(f), the coefficient γ_0 is defined in Eq. (17). The dashed lines in (a)–(c) and (f) are obtained with the tree-level term given in Eq. (12).

For low temperatures ($\beta \to \infty$), only small frequencies contribute to the friction forces and the imaginary part of the polarizability can be approximated as $\mathrm{Im}[\alpha(\omega)] \approx \omega^3[\alpha(0)]^2/(6\pi\epsilon_0 c^3)$. Here, $\alpha(0)$ is the static polarizability of the atom, i.e., the low-frequency limit, where the resonant contribution in Eq. (11) can be neglected. Thus, the blackbody friction coefficient goes as T^8 for small temperatures:

$$\eta_{\mathrm{BB}} \approx \frac{32\pi^5\alpha(0)|^2_{\mathrm{SI}}}{135\hbar^7\epsilon_0^2 c^8\beta^8} = \frac{512\pi^7\alpha(0)|^2_{\mathrm{a.u.}}}{135\alpha^6\hbar m_e^6 c^{14}\beta^8}. \qquad (15)$$

The subscript of the static polarizability indicates the system of units. In atomic units, the subscript a.u. indicates the reduced quantity, i.e., the "numerical value" [26,34]. The polarizability is normally given in atomic units in the literature [35–37]. Assuming that $\mathrm{Im}[(\epsilon(\omega)-1)/(\epsilon(\omega)+1)] \sim \omega/\Omega_0$ for $\omega \to 0$, where Ω_0 is a characteristic frequency of the material, the van der Waals friction coefficient reads as

$$\eta_{\mathrm{QF}} \approx \frac{\pi\alpha(0)|^2_{\mathrm{SI}}}{60\hbar^3\epsilon_0^2 c^3\Omega_0\mathcal{Z}^5\beta^4} = \frac{4\pi^3\hbar^3\alpha(0)|^2_{\mathrm{a.u.}}}{15\alpha^6 m_e^6 c^9\Omega_0\mathcal{Z}^5\beta^4}, \qquad (16)$$

and thus is proportional to T^4 for low temperatures. (The scope of the current paper is restricted to the evaluation of the friction integral (14). Other sources of non-contact atom-wall friction such as a conceivable zero-temperature contribution [38] and [39] or the backreaction by the induced electric field inside the material onto the atom (see Ref. [8]) are not considered here. A more thorough comparison of different sources of van der Waals friction will be presented elsewhere.) For blackbody friction [Figs. 4(a)–4(c)], numerical results are given in terms of the temperature-dependent attenuation time $\tau_{\mathrm{BB}} = m_A/\eta_{\mathrm{BB}}$, where m_A is the mass of the atom (hydrogen or helium). The results for τ_{BB} are free from gauge ambiguities (cf. Figs. 2–4 of Ref. [24]). We also consider the CaF_2 van der Waals friction (for the temperature-dependent dielectric function, see Refs. [40,41]). The numerical results can conveniently be expressed in terms of the damping constant γ_0, where

$$\frac{dv}{dt} = \frac{\eta_{\mathrm{QF}}}{m_A}v, \qquad \frac{\eta_{\mathrm{QF}}}{m_A} = \gamma_0\left(\frac{a_0}{\mathcal{Z}}\right)^5, \qquad (17)$$

and a_0 is the Bohr radius. A reference value at room temperature for metastable helium reads as $\gamma_0^{(\mathrm{He},2^3S)}(298\ \mathrm{K}) = 101.6\ \mathrm{s}^{-1}$, which is exclusively due to the one-loop contribution [second term in Eq. (11)]. The tree-level term given in Eq. (12) contributes $1.82 \times 10^{-5}\ \mathrm{s}^{-1}$ to γ_0 in the mentioned example.

Conclusions.—The imaginary part of the atomic polarizability can be formulated as the sum of a resonant tree-level and a nonresonant one-loop contribution, which behaves as ω^3 for small frequencies [see Eq. (11)]. This

result holds for many-electron atoms; for transparency, the dipole coupling in the derivation outlined here is formulated for a single active electron. The one-loop dominance inverts the perturbative hierarchy of quantum electrodynamics. (The fine-structure constant, which is the perturbative coupling parameter of QED, remains "hidden" in the square of the dynamic dipole polarizability, which is itself proportional to $e^2 = 4\pi\hbar\epsilon_0\alpha$.) The one-loop dominance is tied to the regime of low driving frequencies (on the scale of typical atomic transitions), which are commensurate with thermal photons at typical experimental conditions. It is surprising for a field theory with a small coupling parameter $\alpha \approx 1/137.036 \ll 1$.

Gauge-invariant results are calculated for the blackbody friction, and for CaF_2 van der Waals friction, for ground and selected excited states of hydrogen and helium (Fig. 4). These may be checked against future experimental results. The low-temperature limit of the blackbody and noncontact van der Waals friction is evaluated analytically in Eqs. (15) and (16). In this limit, the coefficients are proportional to the square of the static polarizability, and the friction coefficients are orders of magnitude larger for metastable 2^3S_1 helium than ground-state helium. Our results finally clarify the gauge invariance of the imaginary part of the polarizability [25,42]. The gauge-invariant formulation using asymptotic states confirms that the susceptibility of the atom, for small frequencies, is consistent with the length-gauge expression from Ref. [24] and Chap. XXI of Ref. [25].

This research has been supported by the National Science Foundation (Grants No. PHY-1068547 and No. PHY-1403973) and by the Polish Ministry of Science (MNiSW, Grant No. 0307/IP3/2011/71).

*ulj@mst.edu

[1] L. S. Levitov, Europhys. Lett. **8**, 499 (1989).
[2] V. G. Polevoi, Zh. Eksp. Teor. Fiz. **98**, 1990 (1990) [Sov. Phys. JETP **71**, 1119 (1990)].
[3] J. S. Hoye and I. Brevik, Physica A (Amsterdam) **181A**, 413 (1992); **196A**, 241 (1993).
[4] V. E. Mkrtchian, Phys. Lett. A **207**, 299 (1995).
[5] M. S. Tomassone and A. Widom, Phys. Rev. B **56**, 4938 (1997).
[6] B. N. J. Persson and Z. Zhang, Phys. Rev. B **57**, 7327 (1998).
[7] G. V. Dedkov and A. A. Kyasov, Phys. Lett. A **259**, 38 (1999); Tech. Phys. Lett. **27**, 338 (2001); **28**, 346 (2002); Phys. Solid State **44**, 1809 (2002).
[8] A. I. Volokitin and B. N. J. Persson, J. Phys. Condens. Matter **11**, 345 (1999); Phys. Rev. B **63**, 205404 (2001); **65**, 115419 (2002); **68**, 155420 (2003); Phys. Rev. Lett. **94**, 086104 (2005); Phys. Rev. B **74**, 205413 (2006); Rev. Mod. Phys. **79**, 1291 (2007); Phys. Rev. B **78**, 155437 (2008).
[9] I. Dorofeyev, H. Fuchs, B. Gotsmann, and J. Jersch, Phys. Rev. B **64**, 035403 (2001).
[10] L. P. Pitaevskii and E. M. Lifshitz, *Statistical Physics (Part 2)* (Pergamon Press, Oxford, England, 1958).
[11] R. Kubo, Rep. Prog. Phys. **29**, 255 (1966).
[12] J. B. Pendry, J. Phys. Condens. Matter **9**, 10301 (1997).
[13] T. G. Philbin and U. Leonhardt, New J. Phys. **11**, 033035 (2009); J. B. Pendry, New J. Phys. **12**, 033028 (2010); U. Leonhardt, New J. Phys. **12**, 068001 (2010); J. B. Pendry, New J. Phys. **12**, 068002 (2010).
[14] A. I. Volokitin and B. N. J. Persson, Phys. Rev. Lett. **106**, 094502 (2011).
[15] V. Despoja, P. M. Echenique, and M. Sunjic, Phys. Rev. B **83**, 205424 (2011).
[16] I. L. Singer and H. M. Pollock, *Fundamentals of Friction: Macroscopic and Microscopic Processes* (Kluwer, Dordrecht, 1992); B. N. J. Persson, *Sliding Friction: Physical Principles and Applications* (Springer, Berlin, 1998).
[17] J. A. Sidles, J. L. Carbini, K. J. Bruland, D. Rugar, O. Zuger, S. Hoen, and C. S. Yannoni, Rev. Mod. Phys. **67**, 249 (1995); I. Dorofeyev, H. Fuchs, G. Wenning, and B. Gotsmann, Phys. Rev. Lett. **83**, 2402 (1999); B. Gotsmann and H. Fuchs, Phys. Rev. Lett. **86**, 2597 (2001); B. C. Stipe, H. J. Mamin, T. D. Stowe, T. W. Kenny, and D. Rugar, Phys. Rev. Lett. **87**, 096801 (2001); H. J. Mamin and D. Rugar, Appl. Phys. Lett. **79**, 3358 (2001); P. M. Hoffmann, S. Jeffery, J. B. Pethica, H. Özgur Özer, and A. Oral, Phys. Rev. Lett. **87**, 265502 (2001).
[18] N. Arkani-Hamed, S. Dimopoulos, and G. Dvali, Phys. Lett. B **429**, 263 (1998).
[19] D. Rugar, R. Budakian, H. J. Mamin, and B. W. Chui, Nature (London) **430**, 329 (2004).
[20] E. Buks and M. L. Roukes, Phys. Rev. B **63**, 033402 (2001); H. B. Chan, V. A. Aksyuk, R. N. Kleiman, D. J. Bishop, and F. Capasso, Science **291**, 1941 (2001); Phys. Rev. Lett. **87**, 211801 (2001).
[21] V. Mkrtchian, V. A. Parsegian, R. Podgornik, and W. M. Saslow, Phys. Rev. Lett. **91**, 220801 (2003).
[22] P. A. Maia Neto and C. Farina, Phys. Rev. Lett. **93**, 059001 (2004).
[23] V. Mkrtchian, V. A. Parsegian, R. Podgornik, and W. M. Saslow, Phys. Rev. Lett. **93**, 059002 (2004).
[24] G. Łach, M. DeKieviet, and U. D. Jentschura, Phys. Rev. Lett. **108**, 043005 (2012).
[25] A. Messiah, *Quantum Mechanics II* (North-Holland, Amsterdam, 1962).
[26] H. A. Bethe and E. E. Salpeter, *Quantum Mechanics of One- and Two-Electron Atoms* (Springer, Berlin, 1957).
[27] M. Haas, U. D. Jentschura, and C. H. Keitel, Am. J. Phys. **74**, 77 (2006).
[28] C. Cohen-Tannoudji, B. Diu, and F. Laloë, *Quantum Mechanics*, 1st ed. (J. Wiley & Sons, New York, 1978), Vol. 1.
[29] C. Cohen-Tannoudji, B. Diu, and F. Laloë, *Quantum Mechanics*, 1st ed. (J. Wiley & Sons, New York, 1978), Vol. 2.
[30] Z. C. Yan, J. F. Babb, A. Dalgarno, and G. W. F. Drake, Phys. Rev. A **54**, 2824 (1996).
[31] J. R. Zurita-Sanchez, J.-J. Greffet, and L. Novotny, Phys. Rev. A **69**, 022902 (2004).
[32] T. H. Boyer, Phys. Rev. **182**, 1374 (1969).

[33] L. Novotny and B. Hecht, *Principles of Nano-optics* (Cambridge University Press, Cambridge, England, 2012).
[34] P. J. Mohr, B. N. Taylor, and D. B. Newell, Rev. Mod. Phys. **84**, 1527 (2012).
[35] K. Pachucki and J. Sapirstein, Phys. Rev. A **63**, 012504 (2000).
[36] M. Masili and A. F. Starace, Phys. Rev. A **68**, 012508 (2003).
[37] G. Łach, B. Jeziorski, and K. Szalewicz, Phys. Rev. Lett. **92**, 233001 (2004).
[38] W. L. Schaich and J. Harris, J. Phys. F **11**, 65 (1981).
[39] G. Barton, New J. Phys. **12**, 113045 (2010).
[40] E. D. Palik, *Handbook of Optical Constants of Solids* (Academic, San Diego, CA, 1985).
[41] T. Passerat de Silans, I. Maurin, P. Chaves de Souza Segundo, S. Saltiel, M.-P. Gorza, M. Ducloy, D. Bloch, D. de Sousa Meneses, and P. Echegut, J. Phys. Condens. Matter **21**, 255902 (2009).
[42] G. Łach, M. DeKieviet, and U. D. Jentschura, Phys. Rev. A **81**, 052507 (2010).